Mem. S.A.It. Vol. 94, 167

Memorie della

Rotating stellar populations in NGC 1866

New PARSECv2.0 tracks with rotation

G. Costa[1,2,3] and C. T. Nguyen[4,3]

[1] Physics and Astronomy Department Galileo Galilei, University of Padova, Vicolo dell'Osservatorio 3, I–35122, Padova, Italy
[2] INFN - Padova, Via Marzolo 8, I–35131, Padova, Italy
[3] INAF - Osservatorio Astronomico di Padova, Vicolo dell'Osservatorio 5, I-35122, Padova, Italy
[4] SISSA, via Bonomea 365, I–34136 Trieste, Italy
e-mail: guglielmo.costa@unipd.it

Received:29-10-2022; Accepted: 16-01-2022

Abstract. Stellar rotation affects the evolution of stars in many ways and is a fundamental process that we must include in our models to interpret better stellar observations. In this paper, we present new rotating stellar tracks computed with the PARSEC v2.0 code, and the results of a comprehensive study of the young Large Magellanic Cloud (LMC) cluster NGC 1866. We combined the analysis of the best studied Cepheids of the cluster with a very accurate colour-magnitude diagram (CMD) of it, obtained from the most recent Hubble Space Telescope photometry. Using a Bayesian method based on new PARSEC stellar evolutionary tracks and isochrones with rotation, we obtained a new estimate of the ages and initial rotation velocities of the stellar populations of the cluster. Including all the effects of rotation in our models, such as the gravity darkening, allow us to produce the main characteristics of the Cluster in the CMD (i.e., the extended main-sequence turn-off and the split of the main sequence). Our study reinforces the notion that some young clusters, such as NGC 1866, harbour multiple populations.

Key words. Hertzsprung–Russell and colour–magnitude diagrams – stars: evolution – stars: rotation – stars: variables: Cepheids – galaxies: star clusters: individual: NGC 1866

1. Introduction

In the last decades, several studies have identified stellar rotation as a non-negligible ingredient in stellar evolution (Kippenhahn et al. 1970; Zahn et al. 1992; Meynet et al. 1997; Chieffi et al. 2013, 2017). Already at the beginning of the XX century, theoretical studies found that rotation may affect stars in several ways (VonZeipel et al. 1924). Centrifugal forces may change the stellar structure and its geometry, leading to a departure from spherical symmetry. Moreover, rotation may lead to an enhancement of chemical mixing and mass loss. These processes may be concurrent with other stellar processes, such as core overshooting and stellar winds (Georgy et al. 2013; Jeremyn et al. 2018; Costa et al. 2019a). Rotating stars show different lu-

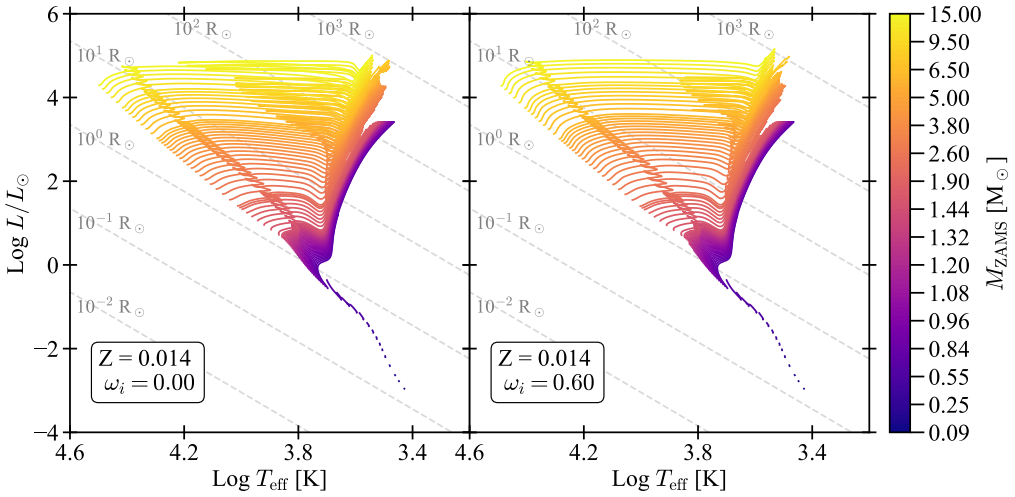

Fig. 1. Selected stellar tracks in the HR diagram with a metallicity content of Z = 0.014, without and with rotation in the left- and right-hand panels, respectively. Different colors indicate the initial mass ($M_{\rm ZAMS}$).

minosities and effective temperatures in the Hertzsprung-Russell (HR) diagram with respect to their non-rotating counterparts. In general, they may have surfaces enriched with products of the CNO cycle at the end of the main-sequence (MS) phase, such as nitrogen (Brott et al. 2011). They live longer in the MS phase and build up bigger He-cores than their non-rotating counterparts, as well as rotation takes to an enhancement in stellar mass loss rate, which lead to a possible impact on their final fate.

In this paper, we briefly review the following works by Costa et al. (2019b) and Nguyen et al. (2022).

2. New stellar tracks and isochrones

PARSEC v2.0 (PAdova-TRieste Stellar Evolution Code, Nguyen et al. 2022) is an updated and revised version of the PARSEC v1.2s code (Bressan et al. 2012), which is used to compute isochrones widely adopted by the astronomical community. This new version adds several input physics updates; in particular, it includes all the main effects of stellar rotation (Costa et al. 2019a,b). These are: the distortions of the structure due to centrifugal forces, by adopting the shellular rotation law; the mixing by the meridional circulation, and shear instability, which transport angular momentum and matter along the star (Meynet et al. 1997); the mass loss enhancement by rotation.

With the new code, we computed several sets of stellar tracks with six initial metallicities: Z = 0.004, 0.006, 0.008, 0.01, 0.014, 0.017, in mass fraction. For each metallicity, we computed sets with several initial rotation rates, $\omega_i = \Omega_i/\Omega_c$ = 0.00, 0.30, 0.60, 0.80, 0.90, 0.95, 0.99, where Ω_i is the initial angular velocity, $\Omega_c = (8\,G\,M_*/27\,R^3_{Pol})^{0.5}$ is the critical angular velocity, G is the gravitational constant, M_* is the total mass of the star and R_{Pol} is the polar radius of the star. Each set contains stars from 0.09 $M_\odot$ to 14 $M_\odot$. All stars begin their evolution from the pre-MS phase and are evolved up to 30 Gyr, or until they reach the early asymptotic giant branch phase, or at the C-exhaustion phase, depending on their initial mass ($M_{\rm ZAMS}$).

All sets of stellar tracks are publicly available in the PARSEC database at the following Web page `http://stev.oapd.inaf.it/PARSEC`. Such tracks are used to construct

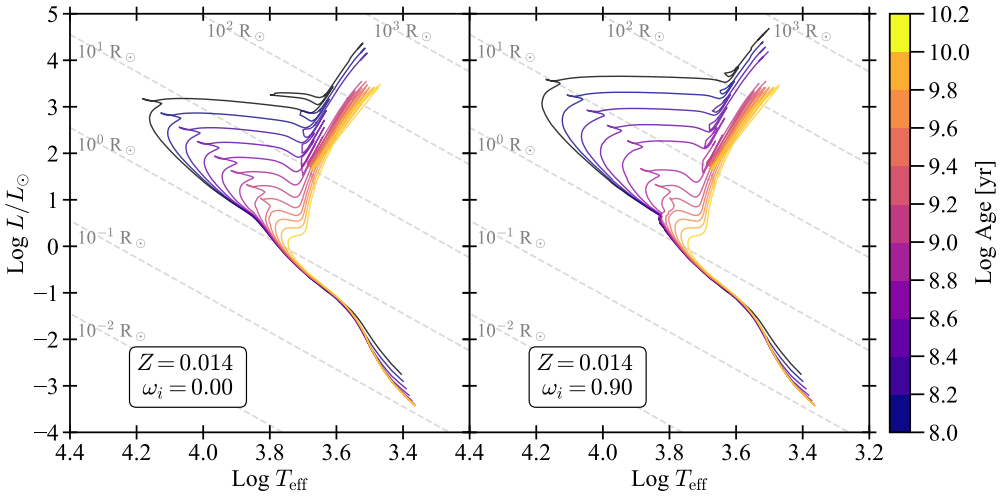

Fig. 2. Selected isochrones in the HR diagram from the new PARSEC database. Non-rotating and rotating isochrones are shown in the left- and right-hand panels, respectively. We selected isochrones with ages from 10^8 to $\sim 15 \times 10^9$ years, indicated in different colors.

the correspondent isochrones, with the TRILEGAL code[1].

Figure 1 shows some sets of selected tracks with and without rotation. Low-mass rotating tracks ($M_{\rm ZAMS} \lesssim 2\ M_\odot$) are colder than the non-rotating ones during the MS phase, whereas intermediate ($2 \lesssim M_{\rm ZAMS} \lesssim 9\ M_\odot$) and massive ($M_{\rm ZAMS} \gtrsim 9\ M_\odot$) stars are both more luminous and colder. Lower effective temperatures are expected, since rotating stars have lower surface effective gravity, leading them to expand and lower their temperature. Higher luminosities are mainly due to enrichment of the stellar surface with helium, brought from the core to the surface by mixing induced by rotation during the MS phase. During the core-helium burning phase, non-rotating intermediate-mass stars have more extended blue loops (in temperature) than rotating stars. As discussed in Costa et al. (2019b), stars that build bigger cores during the MS phase display less extended blue loops, but with higher luminosities. Both the core overshooting process and rotation could lead stars to have larger cores, and careful analysis should be performed to disentangle the effects of the two processes (Costa et al. 2019a).

Figure 2 shows the sets of selected isochrones, without and with rotation (left- and right-panels, correspondingly), in terms of luminosity and effective temperature. The impact of rotation is clearly evidenced, especially around the turn-off region, where a large fraction of the initial rotation rate is still retained. For instance, in the cases of young age, rotating isochrone has a more luminous turn-off with respect to its non-rotating counterpart. The same result holds for the post-MS phases.

For the benefit of comparing with observed data, the isochrones can be coloured with the YBC code (Chen et al. 2019), which includes the gravity darkening effect for rotating stars (VonZeipel et al. 1924; Espinosa et al. 2011; Girardi et al. 2019) (detailed information and examples can be found in Nguyen et al. (2022)).

[1] An online form to compute isochrones with new rotating tracks can be found at `http://stev.oapd.inaf.it/cmd`.

Table 1. On the left-hand part of the table, structural parameters of the Cepheids data, from Marconi et al. (2013), and averaged [Fe/H] data from Lemasle et al. (2017). On the right-hand side, results from the Bayesian analysis.

	Input data				Results		
Name	Mass [$M_\odot$]	log L [$L_\odot$]	$T_{\rm eff}$[K]	[Fe/H]	ω_i	Age [Myr]	[Fe/H]
HV 12197	4.6 ± 0.2	3.045 ± 0.012	5950 ± 12	−0.36 ± 0.03	$0.31^{+0.05}_{-0.16}$	176^{+4}_{-6}	$-0.35^{+0.01}_{-0.02}$
HV 12198	4.2 ± 0.1	3.10 ± 0.01	6050 ± 12	−0.36 ± 0.03	$0.37^{+0.06}_{-0.05}$	176^{+4}_{-6}	$-0.35^{+0.01}_{-0.02}$
HV 12199*	3.5 ± 0.1	2.91 ± 0.01	6125 ± 12	−0.36 ± 0.03	$0.89^{+0.06}_{-0.06}$	288^{+17}_{-23}	$-0.36^{+0.02}_{-0.04}$
We 2	4.31 ± 0.15	3.00 ± 0.01	5925 ± 12	−0.36 ± 0.03	$0.20^{+0.09}_{-0.12}$	176^{+4}_{-6}	$-0.35^{+0.01}_{-0.02}$
V6	4.0 ± 0.1	3.03 ± 0.01	6300 ± 12	−0.36 ± 0.03	$0.18^{+0.11}_{-0.08}$	176^{+4}_{-6}	$-0.35^{+0.01}_{-0.02}$

Columns from left to right show the Cepheids name, mass, luminosity, effective temperature, and iron content from data. Columns 6, 7, and 8, list the best values and 68% credible intervals from Bayesian analysis of the initial rotation rate, age, and iron content.
* For the Cepheid HV 12199 we included just one class of solutions (CS-2) in this table, for a full description of the results, see Costa et al. (2019b).

3. Analysis of NGC 1866 Cepheids and CMD

As the first case of study, we reinterpreted the available data for NGC 1866, in the light of new PARSEC v2.0 stellar models that include rotation. NGC 1866 is a populous young cluster in the Large Magellanic Clouds. Recent photometry provided by the Hubble Space Telescope (HST) revealed the presence of an extended MS turn-off (eMSTO) and a split main sequence (Milone et al. 2017). It contains many evolved stars, with a high number of Cepheid variables (Musella et al. 2016). Fast rotators were also detected directly, around the cluster turn-off, by spectroscopic measurements of line broadening (Dupree et al. 2017). We sought to reinterpret all available data for NGC 1866 by looking at all its features in the CMD. In particular, exploit Cepheids that have accurate pulsational mass determinations.

We analyse the sample of well-studied Cepheids by Marconi et al. (2013) using a Bayesian method, performed with the code PARAM (Rodrigues et al. 2017) and the new rotating PARSEC tracks. From the analysis, we obtain the posterior probability density functions (PDFs) that depend on the metallicity [Fe/H], the age and ω_i of the stars. Table 1 shows the parameters of the selected Cepheids and the results of the Bayesian analysis. From the marginalised 1D-PDFs of age and metallicity of the stars, we find good agreement in both age and metallicity distributions, with the only exception of the Cepheid HV 12199. This star deviates from the trend of the others and seems to be older and more metal-poor. Also, we note that its 1D-PDF in age is clearly bimodal. Excluding HV12199, the combined PDFs (1D-CPDF) of the other Cepheids show a well-defined age peaking at 176 Myr, indicating that they likely belong to the same population. The 2D distribution of age and ω_i, of HV12199 shows two detached regions (or classes) of solutions (see Figure 10 in Costa et al. 2019b). The first (CS-1) peaks at slow initial rotation rates with an age of about 200 Myr and [Fe/H] = −0.40. The second region (CS-2) is centred on high ω_i and older ages ($\sim$ 290 Myr), with a metallicity of [Fe/H] = −0.36. Both solutions give ages different from the common age found for the young Cepheids population. In the CS-1 case, HV12199 is in the central He-burning phase, while the CS-2 case favours a position in the Hertzsprung gap phase.

Figure 3 shows the data of the NGC 1866 cluster. We superimpose the selected

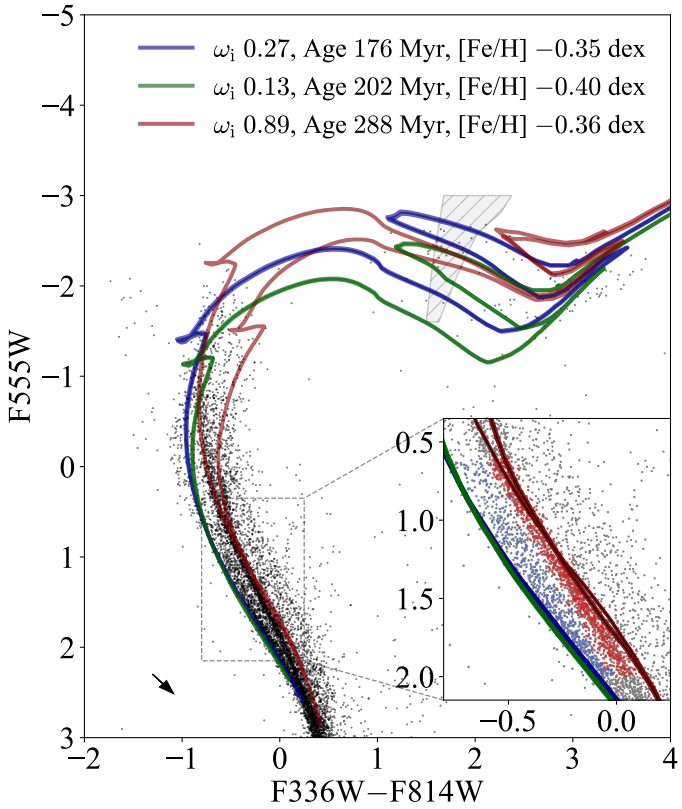

Fig. 3. Comparison in the colour-magnitude diagram between the NGC 1866 cluster data and selected isochrones in the F555W versus F336W - F814W pass-band filters from cameras on board of the Hubble Space Telescope. Data are corrected for the effective magnitude zeropoints for each band, for a true distance modulus of $(m - M)_0 = 18.43$ mag and a foreground extinction of $A_V = 0.28$ mag (Goudfrooij et al. 2018). The black arrow indicates a reddening vector corresponding to $A_V = 0.1$ mag for reference. The gray shaded region indicates the Cepheids instability strip. The luminosity and the effective temperature of the strip are taken from Marconi et al. (2004) and have been coloured with the new YBC bolometric database (Chen et al. 2019). The inset shows a zoom of the MS in which the two main sequences are selected and coloured for indicating the bMS (in blue) and the rMS (in red, Milone et al. 2017). The blue isochrone is selected by taking the best values found from the common age and metallicity of the four-star combined PDF. The green and red isochrones are the two solutions of HV12199, with low (CS-1) and high initial (CS-2) rotation rates, respectively. All the isochrones are plotted with the effect of gravity darkening. The inclination angles, i, are 0° (pole-on) and 90° (edge-on) for the most and less bright isochrones, respectively. This figure is taken from Costa et al. (2019b).

isochrones with ages, metallicities, and initial rotation rates derived from the analysis of the Cepheids properties. The isochrones representing the young Cepheid population nicely reproduce the bluest part of the MS. The isochrone that corresponds to the solution CS-1 reproduces well the blue-MS but does not fit the location of the other four Cepheids simultaneously. Finally, the isochrone selected from the CS-2 solution reproduces the cluster turn-off (due to the gravity darkening effect) and the red-MS very well, but, as can be seen from the inset, the lower red MS is not reproduced perfectly.

4. Conclusions

We have presented the new sets of evolutionary tracks computed with parsec V2.0. In this version of the code, we included the effects of rotation for low-, intermediate-mass and massive stars, with a range of masses from 0.09 $M_{\odot}$ to 14 $M_{\odot}$ and metallicity Z between Z=0.004 and Z=0.017. We computed sets of tracks for seven values of the initial rotation rate in the range ω_i = 0.00 - 0.99. We used the new sets of tracks to study the LMC cluster NGC1866 populations. Analyzing the Cepheids of the cluster, we find the five Cepheids might not belong to the same stellar population. In particular, four Cepheids are harboured in a young slow-rotating population (176^{+4}_{-6} Myr old, $\omega_i \leq 0.4$, and [Fe/H] = $-0.35^{+0.01}_{-0.02}$). While, for the fifth Cepheid (HV12199) we found two different classes of solutions. The first suggests that this Cepheid is hosted in a population of 202^{+3}_{-5} Myr old, initially slowly rotating and with [Fe/H] = $-0.40^{+0.01}_{-0.03}$. The second solution is for an older and initially fast-rotating population (288^{+17}_{-23} Myr, $\omega_i \sim 0.9$, and [Fe/H] = $-0.36^{+0.02}_{-0.04}$). Finally, our results suggest that young clusters like NGC1866 host multiple populations, and to reproduce the characteristics of such clusters (i.e. split-MS and eMSTO), a dispersion in both age and rotation is needed.

This study also suggests a well-defined scenario for the evolution of the cluster. The first older stellar population inherited the initial angular momentum from the progenitor clouds and hosts the largest fraction of fast-rotating stars. Subsequently, after about 130 Myr, another generation of stars is formed out of the gas that has already lost the trace of initial angular momentum. Therefore, stars of this younger generation are mainly slow rotators. Metallicity remains almost unchanged between the populations. Interestingly, this scenario has similarities with the one suggested by Decressin et al. (2007) and Charbonnel et al. (2013), for the formation of multiple populations in old globular clusters.

Acknowledgements. GC acknowledges financial support from the European Research Council for the ERC Consolidator grant DEMOBLACK, under contract no. 770017.

References

Bressan, I. et al. 2012, MNRAS, 427, 127
Brott, I. et al. 2011, A&A, 530, A115
Charbonnel, C. et al. 2013, A&A, 557, L17
Chen, Y., et al. 2019, A&A, 632, A105
Chieffi, A. et al. 2013, ApJ, 764, 21
Chieffi, A. et al. 2017, ApJ, 836, 79
Costa, G. et al. 2019a, MNRAS, 485, 4641
Costa, G. et al. 2019b, A&A, 631, 128
Decressin, T. et al. 2007, A&A, 464, 1029
Dupree, A.K. et al. 2017, ApJL, 846, L1
Espinosa Lara, F., & Rieutord, M. 2011, A&A, 533, A43
Georgy, C. et al. 2013, A&A 558, A103
Girardi, L., et al. 2019, MNRAS, 488, 696
Goudfrooij, P., et al. 2018, ApJ, 864, L3
Jeremyn, A.S. et al. 2018, MNRAS, 480, 5427
Kippenhahn, R. et al. 1970, in IAU Colloq. 4: Stellar Rotation, ed. A. Slettebak, 20
Lemasle, B. et al. 2017, A&A, 608, A85
Marconi, M. et al. 2004, A&A, 417, 1101
Marconi, M. et al. 2013, MNRAS, 428, 2185
Meynet, G. et al. 1997, A&A, 321, 465
Milone, A.P. et al. 2017, MNRAS, 465, 4363
Musella, I. et al. 2016, MNRAS, 457, 3084
Nguyen, C.T. et al. 2022, A&A 665, A126
Rodrigues, T.S. et al. 2017, MNRAS, 467, 1433
VonZeipel, H. et al. 1924, MNRAS, 84, 665
Zahn, J. P. et al. 1992, A&A, 265, 115